APPLIED SCIENCES AND ENGINEERING

Electrodeposited surfaces with reversibly switching interfacial properties

Yue Liu[1], Liyan Zhao[1], Jianjian Lin[2], Shikuan Yang[1]*

Engineered surfaces with reversibly switching interfacial properties, such as wettability and liquid repellency, are highly desirable in diverse application fields but are rare. We have developed a general concept to prepare metallic porous surfaces with exceptionally powerful wettability switch capabilities and liquid-repellent properties through an extremely simple one-step electrochemical deposition process. The wettability switch and manipulative liquid-repellent properties are enabled by orientation change of the dodecyl sulfate ions ionically bonded to the porous membranes during electrodeposition. The porous membrane with adjustable wettability enables it to trap different lubricants on demand within the pores to form liquid-infused porous surfaces with varied liquid-repellent properties. We have demonstrated the application of the (liquid-infused) porous membrane in encryption, controllable droplet transfer, and water harvesting. Moreover, the silver porous membrane can be coated onto a copper mesh, forming a smart antifouling liquid gate capable of allowing water or oil to pass through on request.

INTRODUCTION

Engineered surfaces with reversibly switching interfacial properties, e.g., wettability and liquid repellency, are of great interest in liquid, thermal, as well as analyte and biomarker management–related fields, including microfluidics (*1*), water harvesting and transportation devices (*2*–*5*), separators (*6*), sensors (*7*), and drug delivery systems (*8*). Surfaces with switchable wettability responsive to different stimuli—e.g., light (*9*, *10*), pH value (*11*–*14*), thermal and electrochemical treatment (*15*–*17*), counterions (*18*–*20*), electrical potentials (*21*, *22*), etc.—have been extensively studied. The reversible wettability switch can even be improved from superhydrophilic to superhydrophobic through engineering micro/nanostructures similar to that of lotus leaves (*23*, *24*). Extraordinary liquid-repellent performance has been achieved on the slippery liquid-infused porous surface(s) (SLIPS) modeled after the slippery peristome of the *Nepenthes* pitcher plant (*25*). Stable SLIPS need the porous substrate to trap the lubricant stably inside the pores through surface energy match between the porous substrate and the lubricant. Otherwise, the lubricant will be displaced by the liquid that one wants to repel (*25*). To form SLIPS with different liquids as lubricants, tedious lubricant-dependent surface functionalization processes have to be performed (*25*–*27*). Similarly, most of the existing surfaces with switchable wettability need complex surface functionalization processes (*3*, *21*). Therefore, it is highly desirable to engineer a surface with switchable wettability and a porous substrate capable of accommodating any lubricants to form stable SLIPS without intentional surface functionalization processes. Moreover, multifunctional surfaces with both switchable wettability and liquid-repellent properties are promising for many applications but are rare.

Here, we report an extremely simple one-step electrodeposition approach to fabricate porous metallic surfaces with both robust wettability switch capabilities and outstanding liquid-repellent properties (Fig. 1). Different from the mechanisms of the previously reported wettability switch surfaces, the reversibly tunable wettability of our surface is enabled by the orientation change of the dodecyl sulfate ions ionically bonded to the porous membrane during electrodeposition. When the dodecyl chains point outward, the membrane is superhydrophobic. Electrical potentials can rotate the dodecyl chains to hide inside the pores of the porous membrane, realizing wettability transition from superhydrophobic state to superhydrophilic state. Organic reagents can switch the dodecyl chains to point outward, realizing wettability transition from superhydrophilic state to superhydrophobic state. The above-mentioned orientation change of the dodecyl sulfate ions is confirmed by surface-enhanced Raman scattering (SERS) measurements. The dynamic orientation change of the dodecyl sulfate ions induces the surface energy evolution of the electrodeposited porous surfaces, enabling them to firmly trap different lubricants inside their pores to form different SLIPS with substantially varied liquid-repellent properties. The unprecedentedly complex wetting and liquid-repellent properties of the electrodeposited porous surfaces allow them to be used in encryption, controllable droplet transfer, sensing, and water harvesting fields. Furthermore, the silver porous surfaces can be electrochemically coated onto a copper mesh, which can be used as a smart liquid gate. Selective pass of water or oil through the silver-covered copper mesh can be achieved by forming different SLIPS, realizing high-efficiency water/oil separation. In addition, the electrodeposition method is compatible with sophisticated micro/nanofabrication techniques (*28*), giving rise to the formation of patterned surfaces with reversibly switching interfacial properties. Through systematically analyzing the formation mechanism of the unique electrodeposited multifunctional surfaces, we reveal a general design principle of any porous metallic surfaces with the above-mentioned unique reversibly switching interfacial properties. We envision that our method will have great implications in diverse liquid/thermal-related fields owing to its simplicity (*29*), versatility, and low cost in engineering multifunctional surfaces with unique wetting and liquid-repellent properties, as well as its strong compatibility with sophisticated micro/nanofabrication techniques.

RESULTS

Fabrication and reversible wettability switch of the electrodeposited porous surfaces

Preparation of the silver porous membranes was chosen as an example, which was electrodeposited onto a gold-covered silicon wafer

[1]Institute for Composites Science Innovation, School of Materials Science and Engineering, Zhejiang University, Hangzhou, Zhejiang 310027, China. [2]Key Laboratory of Eco-chemical Engineering, College of Chemistry and Molecular Engineering, Qingdao University of Science and Technology, Qingdao 266042, China.
*Corresponding author. Email: shkyang@zju.edu.cn

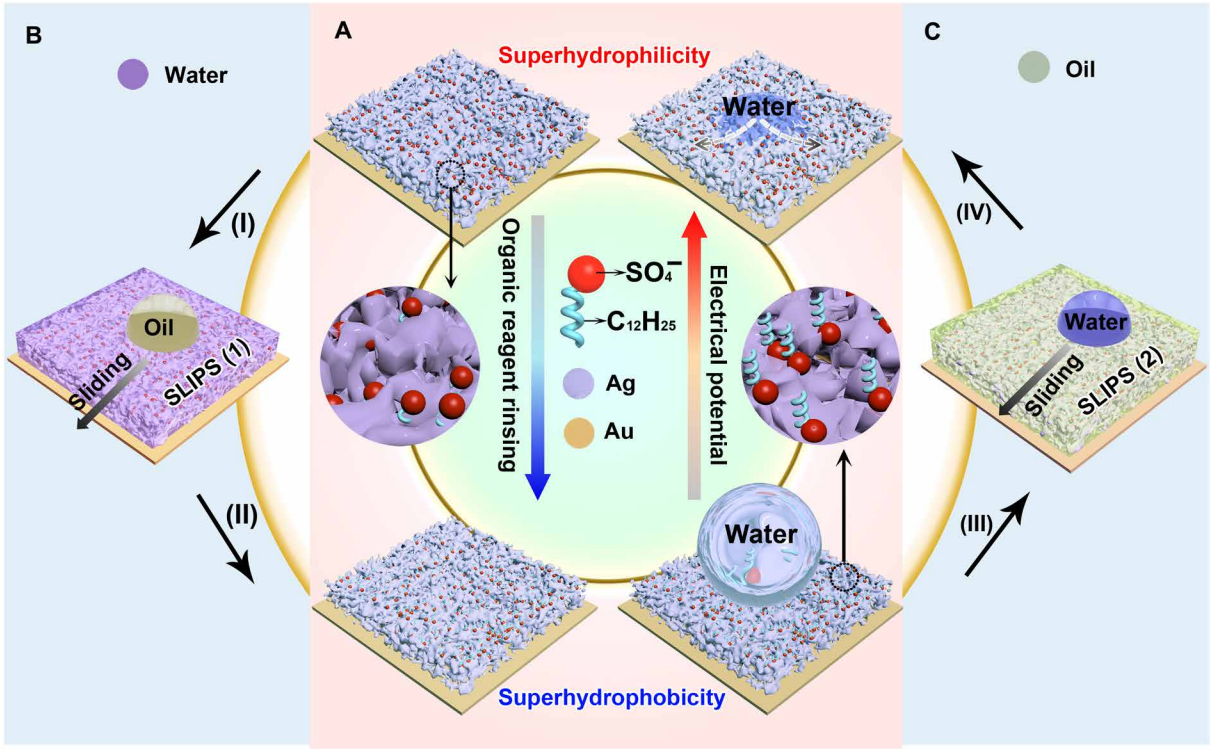

Fig. 1. Reversibly switching wettability and liquid repellency of the electrodeposited silver porous membranes. (**A**) Reversible wettability transition from superhydrophilic to superhydrophobic, enabled by the orientation change of the dodecyl sulfate ions. (**B**) SLIPS 1 is formed by infusing water into the superhydrophilic porous membrane (process I), which can repel oil. After rinsing with ethanol (process II), SLIPS 1 turns superhydrophobic. (**C**) Oil is infused into the superhydrophobic porous membrane (process III), forming SLIPS 2. Water will be repelled by SLIPS 2. The lubricating oil will be released from SLIPS 2 under an electrical potential (process IV), giving rise to a superhydrophilic porous membrane.

in an electrolyte solution composed of 30 mM silver nitrate and 7 mM SDS (Fig. 2A). The roughness of the membrane gradually increased as the electrodeposition time prolonged (Fig. 2B and figs. S1 and S2). The as-prepared membrane was superhydrophilic, as the electrodeposition time was longer than 4 min (Fig. 2C and movie S1). When the deposition time was less than 4 min, the membrane was not thick enough to prohibit the contact between water and the gold substrate. The as-prepared membrane was also superoleophilic, tested by 25 commonly used organic liquids listed in Fig. 2D with a contact angle of ~0° (fig. S3). Unexpectedly, the membranes prepared by electrodeposition for more than 4 min turned superhydrophobic after treatment with organic liquids (movie S2). The superhydrophobicity of the membrane was slightly enhanced as the electrodeposition time prolonged, induced by the slightly increased roughness (Fig. 2C) (*24*). All of the tested 25 commonly used organic liquids could induce the wettability transition from superhydrophilic (superoleophilic) to superhydrophobic (Fig. 2D).

Treatment by water composed of a minute amount of ethanol (e.g., 1% in volume) could turn the membrane from superhydrophilic to superhydrophobic (Fig. 2E). The roll-off angle of the superhydrophobic membrane was generally <4°. The minute amount of ethanol needed for achieving the wettability transition indicated that the wettability of the membrane was highly sensitive to organic reagents. This inspired us to design a gas sensor (fig. S4). It was found that the water contact angle increased as the silver porous membrane was exposed to an ethanol atmosphere. The degree of the water contact angle change for a certain exposure time can reflect the concentration of ethanol.

The superhydrophobic silver porous membrane immediately turned back to being superhydrophilic after being subjected to a negative electrical potential in water. The reversible wettability switch from superhydrophilic to superhydrophobic could be repeated more than 10 times without obvious performance degradation (Fig. 2F). The morphology of the porous membrane was not changed after 10 cycles of wettability transition (Fig. 2G). No chemical and redox reactions took place during the wettability transition process verified by the in situ electrochemical measurements (fig. S5).

Mechanism of the wettability transition

Previous reports have shown wettability transition from (super) hydrophilic to (super)hydrophobic via light irradiation, pH value adjustment, temperature change, and treatment by counterions (*9*–*20*). However, these wetting transition mechanisms cannot be used to explain the wettability switch observed here. The wettability switch process is also quite different from the well-known electrowetting, which only changes the surface from hydrophobic to hydrophilic (*30*, *31*). We performed systematical studies to reveal the underlying mechanism of the wettability transition observed here. Fourier transform infrared spectroscopy (FTIR) and x-ray photoelectron spectroscopy (XPS) measurements proved the existence of dodecyl sulfate ions within the silver porous membrane (fig. S6) (*32*). This is understandable because SDS was used during electrodeposition of the silver porous membrane. Considering the poor solubility of silver sulfate in water, the dodecyl sulfate ions will be ionically bonded to the silver porous membrane, forming a structure similar to the well-studied self-assembled monolayers (*33*). The ionic bonding

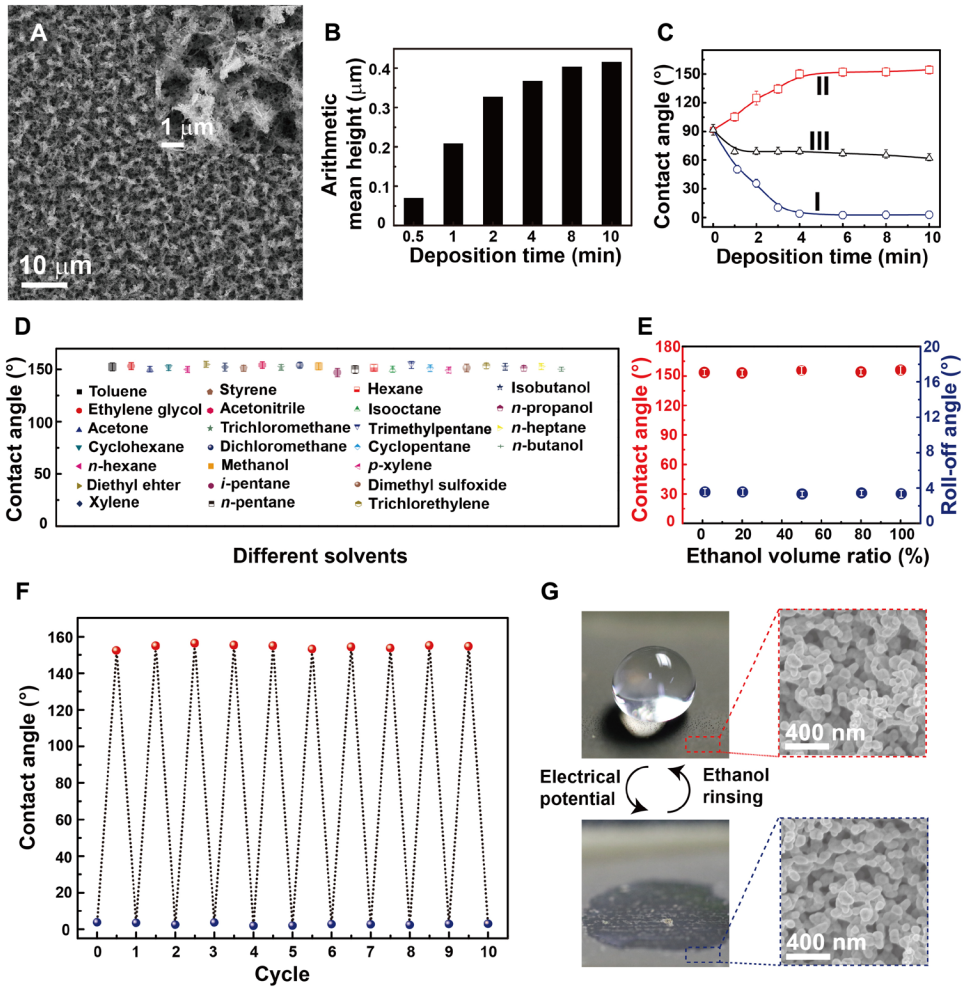

Fig. 2. Fabrication and characterization of the sliver porous membranes. (**A**) Scanning electron microscope image of the electrodeposited silver porous membrane. Inset: Magnified image. (**B**) The arithmetical average roughness height of the silver membranes electrodeposited at 1.5 V for different times. (**C**) Curves I and II are the water contact angles on the as-prepared and the ethanol-treated silver porous membranes prepared at 1.5 V for different times, respectively. Curve III is the water contact angles on the ethanol-treated silver nanoparticle film electrodeposited in pure silver nitrate aqueous solutions. (**D**) The wettability transition from superhydrophilic to superhydrophobic can be completed by treatment with 25 commonly used organic reagents. (**E**) Contact angles and roll-off angles of the superhydrophilic silver porous membrane after being treated by a mixture of water and ethanol at different volume ratios. (**F**) The wettability transition from superhydrophilic to superhydrophobic and back to superhydrophilic for 10 cycles. (**G**) The morphology of the porous membrane is unchanged after 10 cycles of wettability transition. The error bars in (C) to (F) are obtained on the basis of at least five independent measurements.

between dodecyl sulfate ions and silver was proven by the existence of the 963-cm^{-1} SERS peak from the silver porous membrane (Fig. 3A), which originated from silver sulfate (*34*, *35*).

On the basis of the above experimental results, we proposed the molecular orientation change mechanism of the wettability switch of the silver porous membrane (Fig. 1). The dodecyl chain tails will hide inside the pores of the freshly prepared silver porous membrane because of their hydrophobicity. Therefore, the as-electrodeposited silver porous membranes demonstrate a superhydrophilic property, which originated from the exposed hydrophilic sulfate heads. When the superhydrophilic surface is exposed to organic reagents (e.g., ethanol), the hidden dodecyl chain tails will be pulled out and change their orientation because of the strong affinity between the dodecyl chain tails and the organic liquids. These exposed dodecyl chain tails render the superhydrophobicity of the silver porous membrane. Under a negative electrical potential, the dodecyl chain tails will be positively charged (Fig. 3B) (*36*). Therefore, the positively charged dodecyl chain tails will move toward the negatively charged silver porous membrane, achieving orientation change of the dodecyl chain tails (Fig. 3B). The dodecyl chain tails at different heights of the silver porous membrane change their orientation in sequence, giving rise to a gradual wettability transition from superhydrophobic to superhydrophilic (Fig. 3B).

It is challenging to prove the orientation change of the dodecyl chains on the rough porous membranes using a conventional scanning tunneling microscope or an atomic force microscope that are only applicable to ultrasmooth surfaces. Therefore, we used SERS technique capable of providing fingerprint information of even single molecules to prove/monitor the orientation change of the dodecyl chains on the silver porous membranes (*7*, *34*, *37*, *38*). The dodecyl sulfate ions were ionically bonded to the silver porous membrane (Fig. 3A). Therefore, the distance between the sulfate ions and the SERS-sensitive sites (known as hot spots) existing within the pores of the silver porous membrane should not be changed (Fig. 3C)

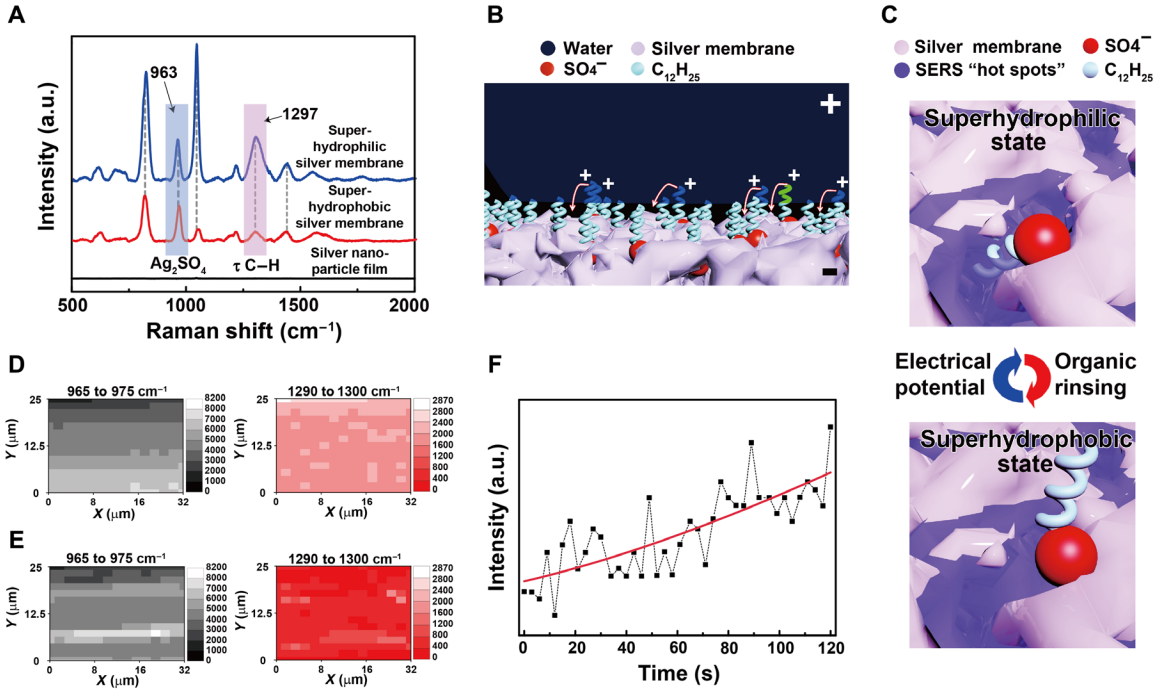

Fig. 3. Mechanism of the reversibly switching interfacial properties. (**A**) SERS spectra of the silver porous membrane at superhydrophilic state and superhydrophobic state and the electrodeposited silver nanoparticle film in pure silver nitrate aqueous solutions. The SERS peaks located at 963 and 1297 cm^{-1} are assigned to silver sulfate and the torsional vibration mode (τ) of C—H in the dodecyl chains, respectively. a.u., arbitrary units. (**B**) Schematic illustration of the orientation change of the dodecyl chains under an electrical potential. Positive charges will accumulate at the tips of the dodecyl chains contacting water, rotating them toward the negatively charged silver porous membrane. (**C**) Schematic illustration of the SERS intensity evolution of the dodecyl chains at different wetting states. At hydrophilic state, dodecyl chains are exposed to the SERS "hot spots" existing within the pores of the silver membrane, resulting in strong SERS signals. At hydrophobic state, the dodecyl chains are far away from the SERS hot spots, demonstrating weak SERS signals. (**D** and **E**) The SERS mapping results of silver sulfate and the dodecyl chains when the porous membrane is superhydrophilic and superhydrophobic, respectively. (**F**) The intensity evolution of the 1297-cm^{-1} SERS peak from dodecyl chains at a specific location as the electrical potential was applied to the superhydrophobic silver porous membrane (photo credit: Yue Liu, Zhejiang University).

(*34*, *37*, *38*). In turn, the intensity of the SERS peak from the silver sulfate should not be prominently influenced by the orientation change of the dodecyl chains. However, the distance between the dodecyl chains and the SERS hot spots changes prominently as the orientation of the dodecyl sulfate ions varies (Fig. 3C). In turn, the SERS intensity of dodecyl chains should vary as their orientation changes. Therefore, the ratio of the SERS intensity between dodecyl chains and silver sulfate can be used to prove the orientation change of the dodecyl sulfate ions.

When the porous membrane is at the superhydrophilic state, the dodecyl chains are hidden inside the pores where SERS hot spots are located (Fig. 3C) (*34*, *37*, *38*). Therefore, extremely strong SERS signals of dodecyl chains were observed. The intensity ratio between the 1297-cm^{-1} SERS peak from dodecyl chains and the 963-cm^{-1} SERS peak from the silver sulfate reaches 1.02 (Fig. 3A). In contrast, the intensity ratio decreased to be about 0.18 when the porous membrane is at the superhydrophobic state (Fig. 3A). Although the ratio changes at different sites on the silver porous membrane, the ratio is always much higher when the membrane is superhydrophilic than when the membrane is superhydrophobic (fig. S7A).

SERS mapping measurements further confirmed the molecular orientation change mechanism (Fig. 3, D and E). Strong SERS signals of silver sulfate were observed over the mapping area regardless of whether the membrane is at the superhydrophilic or at the superhydrophobic state. As expected, stronger SERS signals of dodecyl chains were observed when the membrane was at the superhydrophilic state than at the superhydrophobic state (Fig. 3, D and E). SERS mapping measurements on the superhydrophobic silver porous membrane after electrical potential treatment for prolonged times demonstrated that the SERS intensity of dodecyl chains gradually increased, while that of the silver sulfate remained almost unchanged (fig. S7, B to D).

The SERS intensity of the dodecyl chains was in situ monitored at a fixed position on the silver porous membrane under electrical potential treatment. As anticipated, the SERS intensity of the dodecyl chains gradually increased as the superhydrophobic silver porous membrane was switched to hydrophilic under the electrical potential treatment (Fig. 3F).

The above SERS results have conclusively proven that the wettability switch of the silver porous membranes is caused by the orientation change of the dodecyl sulfate ions. The detailed process of the orientation change of the dodecyl sulfate ions needs further studies. Notably, the molecular orientation change mechanism is different from the molecular conformation change mechanism reported before (*21*). In the latter case, the hydrophobic state is achieved through bending the alkyl chains using an electric potential. Therefore, the hydrophobic surface will turn hydrophilic as the electrical potential is removed.

To further emphasize the importance of the dodecyl sulfate ions to the wettability transition, we prepared silver nanoparticle films by electrodeposition in the electrolyte without the addition of SDS (Fig. 3A and fig. S8). As anticipated, the wettability transition was not observed in the silver nanoparticle film without the dodecyl sulfate

ions (curve III in Fig. 2C). Furthermore, when the dodecyl chains were removed by the oxygen plasma treatment (*35*), the silver porous membrane also lost the wettability switch capability.

Design rationale

The stable ionic bonds within silver sulfate prohibit the detachment of dodecyl sulfate ions from the silver porous membrane during their orientation change. As expected, similar reversible wetting transition was observed from the electrodeposited lead/lead oxide coatings owing to the insolubility of lead sulfate (fig. S9). However, this kind of wetting transition was absent in the electrodeposited porous copper membranes owing to the solubility of copper sulfate (fig. S9). This reveals that one design principle to engineer surfaces with switchable wettability on other metals is to choose surfactants with their acidic ions capable of forming insoluble salts with the corresponding metal ions. The chain length of the surfactant used has prominent influence on the wettability transition performance of the electrodeposited porous membranes. The reversible wettability switch was still observable when we replaced SDS with sodium 1-octanesulfonate in the electrolyte solution. However, no wettability transition was observed when sodium hexane-1-sulphonate was used in the electrolyte solution (fig. S10). Therefore, the alkyl chain in the surfactant should be composed of more than six carbon atoms to realize the reversible wettability transition. Through engineering surfactants with

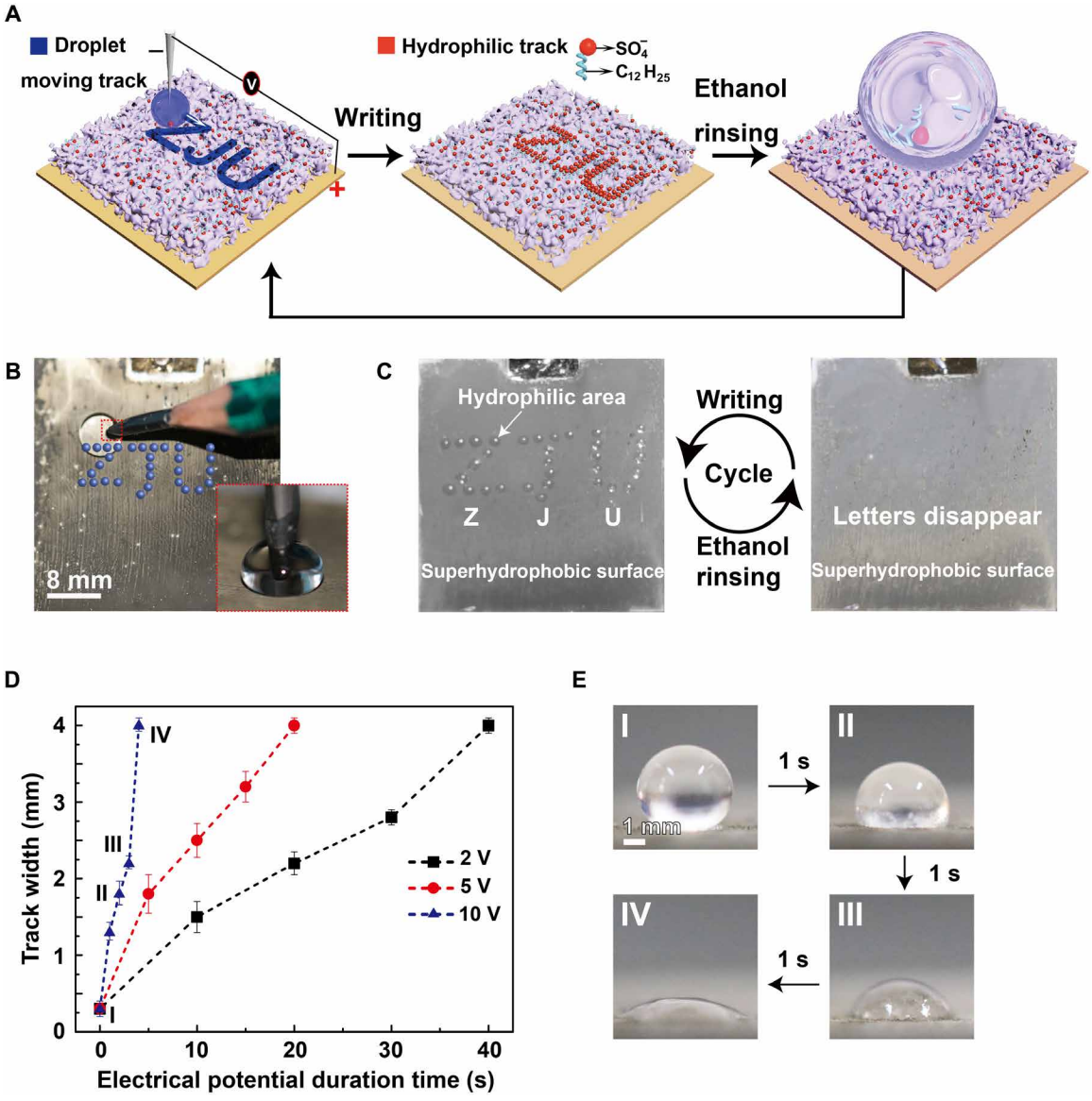

Fig. 4. Application in encryption. (**A**) Schematic of the information encryption process. A water droplet is dragged by a pencil connected to the negative pole of a power supply to write letters ZJU on the superhydrophobic surface connected to the positive pole of the power supply. The track turns hydrophilic. When the porous membrane is immersed in water or exposed to water steam, the ZJU letters will appear. Ethanol rinsing can turn the hydrophilic track superhydrophobic, allowing for repeatable usage. (**B**) The setup for the encryption application. Inset: A pencil behaving as a cathode immersed in a droplet sitting on the superhydrophobic surface. (**C**) Repeatable usage of the silver porous membrane in encryption applications. (**D**) The track width as a function of the duration time at 2, 5, and 10 V. The error bars are obtained on the basis of five independent measurements. (**E**) Photographs of the track created at 10 V for different times (photo credit: Yue Liu, Zhejiang University).

appropriate acidic heads and perfluorinated chain tails, electrodeposited porous membranes with reversible wettability transition from superhydrophilic to superoleophobic are expected.

Overall, we have developed a new concept to realize reversible wettability switch through varying the orientation of the surfactant ions ionically bonded to a metallic porous membrane. This concept can guide the design of diverse material systems with reversibly switching interfacial properties using a simple one-step electrodeposition approach. This kind of metallic coatings can be conformally electrodeposited onto any conductive substrates or even conductive meshes, as discussed below. Moreover, the electrodeposition method used to fabricate the porous membranes is compatible with sophisticated micro/nanostructure fabrication techniques. For example, patterned silver porous membranes could be prepared by electrodeposition under the protection of a mask. The wettability of the patterned porous membranes is also reversibly switchable (fig. S11).

Encryption

The ethanol-treated superhydrophobic silver porous membranes were used in information encryption (Fig. 4 and fig. S12). A pencil behaving as cathode electrode immersed in a droplet sitting on the superhydrophobic surface was used to drag the droplet to write the letters "ZJU." The invisible ZJU track would become hydrophilic (Fig. 4, A to C). When the surface was exposed to water steam or was immersed in water, water droplets would attach onto the hydrophilic ZJU track, demonstrating the encrypted information (Fig. 4C). The hydrophilic track could be immediately and permanently removed by ethanol rinsing, allowing the porous membrane to be used multiple times (Fig. 4C). The hydrophilicity and the width of the hydrophilic track were dependent on the writing speed (Fig. 4, D and E). For example, the dwell time of the droplet to make the membrane surface underneath superhydrophilic was around 40 s at 2 V. In contrast, the dewell time would be shortened to <10 s when the applied potential was increased to 10 V (Fig. 4D). Under 10-V potential, the writing speed could be close to the normal writing speed.

Similarly, a mask with ZJU letters was attached onto the as-prepared superhydrophilic silver porous membrane before spraying ethanol onto the surface. Subsequently, the ZJU letters would become superhydrophobic (fig. S13). No water would appear onto the ZJU letters when the surface was exposed to water steam or was immersed in water, conveying the encrypted information.

Droplet transfer

Considering the strong (weak) adhesion of water droplets on the superhydrophilic (superhydrophobic) surface, droplet transfer was realized using the ethanol-treated superhydrophobic silver porous membrane (fig. S14). A superhydrophobic porous membrane connected to the negative pole was approaching a water droplet sitting on the other superhydrophobic porous membrane connected to the positive pole of a power supply. The interface between the water droplet and the top superhydrophobic membrane would become hydrophilic (Fig. 4E). Then, the droplet would adhere to the top silver membrane and could be transferred onto another substrate.

Liquid-repellent properties

According to previous studies, the formation of stable SLIPS needs an energy match between the porous substrate and the infused lubricant (*25*). The as-prepared superhydrophilic porous membrane could trap water inside the pores, forming water-infused SLIPS 1. SLIPS 1 could repel oils immiscible with water with a contact angle hysteresis of ~0.15° (Fig. 5A and movie S3). SLIPS 1 became superhydrophobic when rinsed with organic reagents miscible with water

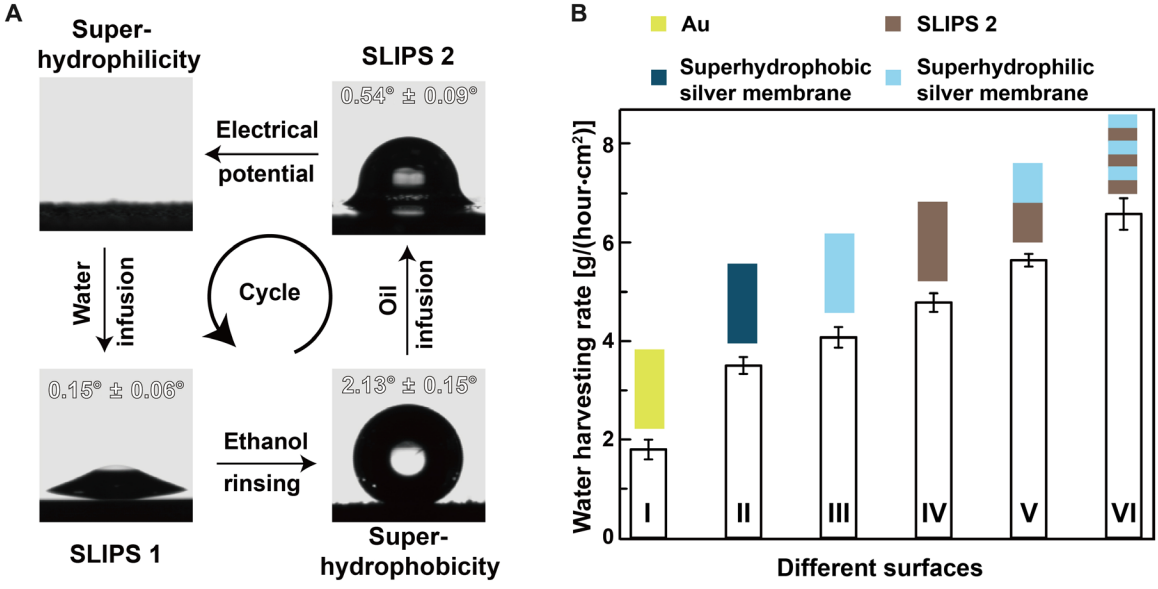

Fig. 5. Reversibly switching interfacial properties and applications in fog harvesting. (**A**) Optical images of a water droplet sitting on the (liquid-infused) porous membranes at different states. Inset: The value of the contact angle hysteresis. The as-prepared superhydrophilic porous membrane can form SLIPS 1 by infusing water. SLIPS 1 turns superhydrophobic after ethanol rinsing. Oil can be infused into the superhydrophobic porous membrane, giving rise to the formation of SLIPS 2. SLIPS 2 can turn back to being superhydrophilic under an electrical potential treatment. This cycle can repeat for multiple times. (**B**) The water harvesting rate for different surfaces. Surface I, gold film; surface II, superhydrophobic silver porous membrane; surface III, superhydrophilic silver porous membrane; surface IV, SLIPS 2; surface V, the top half surface is superhydrophilic and the bottom half surface is SLIPS 2; surface VI, the surface composed of alternatively arranged superhydrophilic surface and SLIPS 2. The error bars are obtained on the basis of three independent measurements.

(e.g., ethanol) (Fig. 1). In turn, the ethanol-treated superhydrophobic porous membrane could trap oils inside the pores, forming oil-infused SLIPS 2. SLIPS 2 could repel water with a contact angle hysteresis of ~0.54° (movie S4). SLIPS 2 could also be formed by directly infusing the oil lubricants into the as-prepared silver porous membrane because it is superoleophilic. When SLIPS 2 was treated by a negative electrical potential in water, the dodecyl chain tails would hide inside the porous structures again. Then, the trapped oil would be released from the porous membrane, leaving behind the superhydrophilic porous membrane (Fig. 5A). In short, the silver porous membrane could change from superhydrophilic, to SLIPS 1, to superhydrophobic, to SLIPS 2, and further back to superhydrophilic, forming a cycle. The cycle could be repeated for desired times. The porous surfaces with such a complex wetting and liquid-repellent properties have never been reported before. Notably, this is the first demonstration of fabricating different kinds of SLIPS using the same porous membrane via dynamically adjusting its wettability to match different lubricants.

Fog harvesting

To obtain high fog harvesting efficiency, it is crucial to balance the water nucleation tendency and the water repellency of a surface (*27*). Water molecules prefer to adhere to and nucleate on hydrophilic surfaces. However, it is difficult for water drops to slide on hydrophilic surfaces because of the strong adhesion force between water and the hydrophilic surface. Even the superhydrophobic surface will get flooded during water harvesting (*39*), giving rise to a low droplet removal efficiency. Inspired by the Namib desert beetle, using patterned hydrophilic elytra to capture water droplets and the hydrophobic elytra to make the droplets roll off (*40*), we patterned stripes of SLIPS 2 with an excellent water droplet repellency capability by spraying lubricant though a mask on a superhydrophilic silver porous membrane (Fig. 5B and fig. S15). Water molecules can adhere to and nucleate on the superhydrophilic stripes when exposed to a water mist. When the large water drops formed in the superhydrophilic area moved onto the area of SLIPS 2, they immediately rolled off from the surface. As anticipated, the porous membrane with hybridized wettability and water repellency demonstrated an outstanding fog harvesting efficiency (Fig. 5B).

Smart liquid gate

The silver porous membrane was electrochemically coated onto a copper mesh, which was used as a smart liquid gate (Fig. 6). The original superhydrophobic copper mesh prohibited the pass-through of water. When the copper mesh was subjected to a negative electrical potential, it became superhydrophilic and immediately allowed

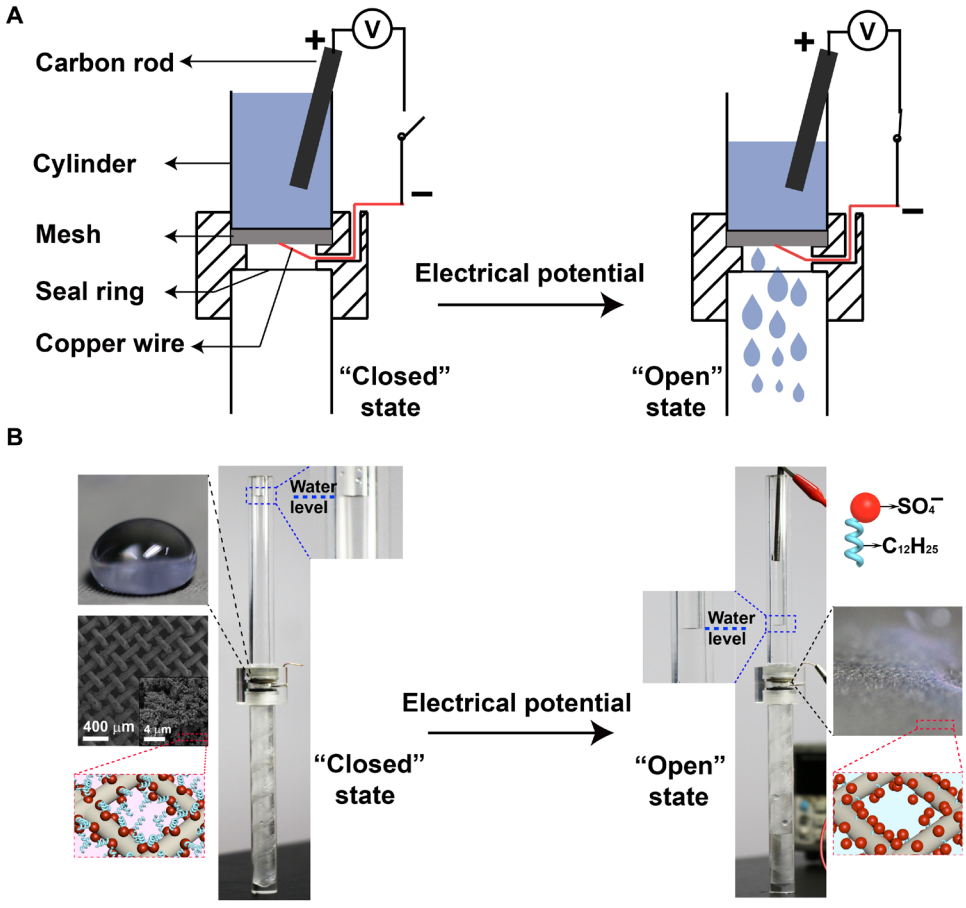

Fig. 6. Application as a smart liquid gate. (**A**) Schematic of the setup of the smart liquid gate. (**B**) At the beginning, the mesh is at the "closed" state because the silver-coated copper mesh is superhydrophobic. Once the mesh is triggered by an electrical potential, it turns to the "open" state, and water starts to pass through the mesh. Inset: The image of a water droplet on and the orientation of the dodecyl sulfate ions on the silver-coated copper mesh at the closed and the open state, as well as the microstructure of the silver-coated copper mesh (photo credit: Yue Liu, Zhejiang University).

water to pass through. The superhydrophilic mesh could be changed into superhydrophobic after being exposed to ethanol vapor for recycle usage.

Water/oil separation

Conventional porous membranes used for water/oil separation allow either water or oil to pass through (*4*). Here, the silver-coated porous copper mesh can selectively allow water or oil to pass through by forming different SLIPS (Fig. 7, A and B). SLIPS 2 was formed by infusing oil (e.g., cyclohexane) into the pores of the superhydrophobic silver-coated copper mesh (process I in Fig. 7A). SLIPS 2 only allowed cyclohexane to pass through, leaving behind water (Fig. 7B). The left water could easily slide away from SLIPS 2, achieving separation of cyclohexane from water. Electrical potential could release cyclohexane from SLIPS 2. Then, water could be trapped within the pores of the superhydrophilic silver-coated porous copper mesh, forming SLIPS 1. SLIPS 1 allowed water to pass through, leaving behind cyclohexane (Fig. 7B). SLIPS 1 could be changed to SLIPS 2 by ethanol rinsing and infusing oil lubricant (process III and process I in Fig. 7A). SLIPS 2 could be changed into SLIPS 1 after being subjected to an electrical potential and infusing water, as mentioned above (process II in Fig. 7A). The transition from SLIPS 1 to SLIPS 2 can be repeated for desired times without influencing the oil/water separation efficiency. For example, the separation efficiency was still ~98% even after five times of transition between SLIPS 1 and SLIPS 2 (Fig. 7C). Therefore, water and oil could selectively pass through the silver-coated copper mesh via engineering different SLIPS, different from existing water/oil separators. The SLIPS 1 (or SLIPS 2) could prohibit contamination from oil (or water) owing to its excellent oil (or water) repellency (*41*).

DISCUSSION

In summary, we have developed a general concept to engineer metallic coatings with switchable wettability and liquid-repellent properties via an extremely simple one-step electrodeposition process. The orientation change of the dodecyl sulfate ions ionically bonded to the electrodeposited porous metallic membrane triggered by organic reagent treatment, or an external electrical potential enables the wettability switch. The as-prepared silver porous membrane is superhydrophilic, with the dodecyl chains hidden inside the pores. The superhydrophilic porous membrane turns superhydrophobic when it is exposed to common organic reagents that can change the orientation of the dodecyl chains. The superhydrophobic silver

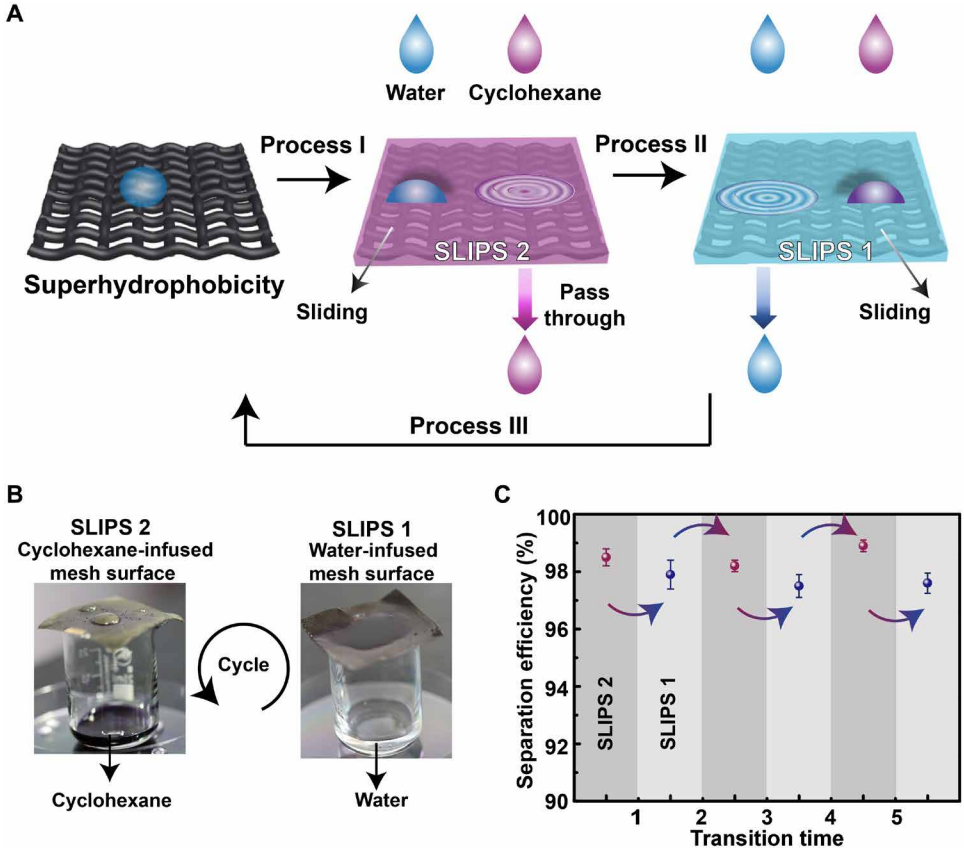

Fig. 7. Selective water/oil separation. (**A**) Schematic illustration of the working mechanism of the water/oil separator. Process I: Infusing oil (here, cyclohexane) into the superhydrophobic porous membrane to form SLIPS 2. SLIPS 2 only allows cyclohexane to pass through; water will be left behind and slide away easily from SLIPS 2. Process II: When SLIPS 2 is subjected to an electric potential, the lubricating oil will be released from the porous surface. SLIPS 2 will turn superhydrophilic. The superhydrophilic porous membrane can trap water to form SLIPS 1. SLIPS 1 only allows water to pass through, while oil will be left behind and slide away from SLIPS 1. Process III: SLIPS 1 will turn superhydrophobic after being treated with ethanol. Processes I, II, and III form a cycle and can be repeated for desired times. (**B**) SLIPS 2 allows dyed cyclohexane to pass through, leaving behind water. SLIPS 1 allows water to penetrate, leaving behind dyed cyclohexane. (**C**) The oil/water separation efficiency of SLIPS 1 and SLIPS 2 at different transition times (photo credit: Yue Liu, Zhejiang University).

porous membrane can return to being superhydrophilic when triggered by an external electrical potential. The wettability transition can be repeated more than 10 times. The switchable wettability allows the porous membrane to trap different lubricants, resulting in different SLIPS. The porous membrane can be changed from superhydrophilic, to water-infused SLIPS, to superhydrophobic, to oil-infused SLIPS, and further back to superhydrophilic, forming a cycle. We have demonstrated the application of the (liquid-infused) porous membrane with reversibly switching wettability in encryption, droplet transfer, sensing, and water harvesting fields. Furthermore, the silver membrane can be deposited onto a copper mesh, forming a smart liquid gate capable of allowing water to pass through when triggered by an electrical potential. The silver-coated copper mesh can allow water or oil to pass through on request by forming water- or oil-infused SLIPS, realizing highly efficient water/oil separation. We have demonstrated a general and extremely simple approach toward engineering metallic coatings with switchable wettability and liquid-repellent properties, which has promising applications in liquid and heat management–related fields.

MATERIALS AND METHODS

Electrodeposition of porous membranes

For simplicity, the silver porous membrane was electrodeposited using a two-electrode setup. The anode was a carbon rod with a diameter of ~3 mm. The cathode was a piece of gold-coated silicon wafer or copper mesh (with an average pore diameter of about 115 μm) with an area of ~1 cm by 1 cm. The deposition voltage was 1.5 V, unless otherwise specified. The silver porous membrane was electrodeposited for 10 min, unless otherwise specified. The electrolyte was composed of 30 mM silver nitrate and 7 mM SDS. Two volts was used to change the silver porous membrane from superhydrophobic to superhydrophilic. For comparison, pure silver nanoparticle films were electrodeposited at 1.5 V for 10 min in silver nitrate aqueous solution at a concentration of 30 mM. The deposition was performed at room temperature (~25°C). The deposition voltage for lead/lead oxide was 5 V for 10 min. The electrolyte was composed of 15 mM lead acetate trihydrate and 7 mM SDS. Electrodeposition of copper was performed at 3 V for 20 min in an electrolyte solution composed of 15 mM copper nitrate trihydrate and 7 mM SDS.

Characterization

The microstructure of the porous membranes was studied using an x-ray diffraction spectrometer (D/Max 2550pc). The morphology of the porous membranes was observed with a scanning electron microscope (Hitachi SU-8010) operating at 5.0 kV. The roughness of the porous membrane was determined with a laser scanning confocal microscope (KEYENCE Corporation, VK-X1000). The wetting and liquid-repellent properties were evaluated using a goniometer (OCA 20, Germany). The electrochemical measurements were performed on a CHI 760E electrochemical workstation (CH Instruments Inc., Shanghai) in a three-electrode configuration. SERS measurements were performed on a confocal Raman microscopic system (LabRAM HR Evolution, France). The excitation wavelength was 633 nm generated by an Nd:yttrium-aluminum-garnet laser operating at a power of about 0.25 mW. SERS mapping measurements were carried out over an area of 32 μm by 25 μm. The accumulation time for the SERS signals was 10 s. FTIR and XPS measurements were carried out on a Nicolet 5700 FTIR spectrometer and an Axis Supra XPS spectrometer, respectively.

Sensor

A certain volume of ethanol was introduced into a sealed chamber. The volume ratio between ethanol and the chamber was referred as ethanol volume ratio shown in Fig. 2E and fig. S4. Then, the as-prepared porous membrane was exposed to the ethanol environment for 3 min. The water contact angle was then measured on the porous membrane.

Fog harvesting

The cool mist was produced by a conventional ultrasonic humidifier. The average size of the droplet was about 3 μm. The mist flowed directly toward the surfaces placed vertically. The outlet of the mist was facing the surfaces at a distance of ~5 cm. The water dropping down from the surfaces was collected with a clean cup. Then, the fog harvesting efficiency was calculated on the basis of the weight of the water collected at different time intervals.

Smart liquid gate and water/oil separation

A piece of silver-coated copper mesh was placed at the connection area of two cylinders. A copper wire was connected to the copper mesh. The copper mesh was connected to the negative pole, while a carbon rod immersed in water was connected to the positive pole of a power supply. At the beginning, water cannot pass through the superhydrophobic copper mesh. Triggered by a negative electrical potential, water started to pass through the copper mesh, working as a smart liquid gate. If the silver-coated copper mesh was infused with water, then SLIPS 1 would form. SLIPS 1 only allowed water to pass through while leaving behind oil. If the silver-copper mesh was infused with oil (e.g., cyclohexane), then SLIPS 2 would form. Only oil could pass through SLIPS 2, leaving behind water. The separation efficiency was calculated by the weight of the collected liquid in the beaker over the weight of the same liquid applied onto the separator.

SUPPLEMENTARY MATERIALS

Supplementary material for this article is available at http://advances.sciencemag.org/cgi/content/full/5/11/eaax0380/DC1

Fig. S1. Characterization of the silver porous membrane.
Fig. S2. Roughness characterization of the electrodeposited silver porous membranes.
Fig. S3. An optical image of an oil droplet (here, lubricant Krytox 102 obtained from DuPont, USA) spreading on the as-prepared silver porous membrane.
Fig. S4. Sensing of ethanol.
Fig. S5. Cyclic voltammetry measurement.
Fig. S6. XPS characterization.
Fig. S7. SERS mapping results.
Fig. S8. No wettability switch was observed on the electrodeposited pure silver nanoparticle film.
Fig. S9. Design rationale of the electrodeposited membranes with reversibly switching interfacial properties.
Fig. S10. The effect of the alkyl chain length on the wettability transition performance.
Fig. S11. Compatibility of the electrodeposition method to the sophisticated micro/nanofabrication techniques.
Fig. S12. Schematic illustration of the setup used in information encryption application.
Fig. S13. Creating superhydrophobic tracks on a superhydrophilic silver porous membrane.
Fig. S14. Droplet transfer.
Fig. S15. Water harvesting performance on different surfaces.
Movie S1. The superhydrophilicity of the as-electrodeposited silver porous membrane.
Movie S2. The superhydrophobicity of the organic reagent–treated silver porous membrane.
Movie S3. The repellency of oil droplets of SLIPS 1.
Movie S4. The repellency of water droplets of SLIPS 2.

REFERENCES AND NOTES

1. D. L. Huber, R. P. Manginell, M. A. Samara, B.-I. Kim, B. C. Bunker, Programmed adsorption and release of proteins in a microfluidic device. *Science* **301**, 352–354 (2003).
2. M. Liu, S. Wang, L. Jiang, Nature-inspired superwettability systems. *Nat. Rev. Mater.* **2**, 17036 (2017).
3. B. Xin, J. Hao, Reversibly switchable wettability. *Chem. Soc. Rev.* **39**, 769–782 (2010).
4. K. Li, J. Ju, Z. Xue, J. Ma, L. Feng, S. Gao, L. Jiang, Structured cone arrays for continuous and effective collection of micron-sized oil droplets from water. *Nat. Commun.* **4**, 2276 (2013).
5. D. Quéré, Wetting and roughness. *Annu. Rev. Mater. Res.* **38**, 71–99 (2008).
6. X. Hou, Y. Hu, A. Grinthal, M. Khan, J. Aizenberg, Liquid-based gating mechanism with tunable multiphase selectivity and antifouling behaviour. *Nature* **519**, 70–73 (2015).
7. S. Yang, X. Dai, B. B. Stogin, T.-S. Wong, Ultrasensitive surface-enhanced Raman scattering detection in common fluids. *Proc. Natl. Acad. Sci. U.S.A.* **113**, 268–273 (2016).
8. P. Gupta, K. Vermani, S. Garg, Hydrogels: From controlled release to pH-responsive drug delivery. *Drug Discov. Today* **7**, 569–579 (2002).
9. K. Ichimura, S.-K. Oh, M. Nakagawa, Light-driven motion of liquids on a photoresponsive surface. *Science* **288**, 1624–1626 (2000).
10. G. Kwon, D. Panchanathan, S. R. Mahmoudi, M. A. Gondal, G. H. McKinley, K. K. Varanasi, Visible light guided manipulation of liquid wettability on photoresponsive surfaces. *Nat. Commun.* **8**, 14968 (2017).
11. Y. Liu, M. Zhao, D. E. Bergbreiter, R. M. Crooks, pH-switchable, ultrathin permselective membranes prepared from multilayer polymer composites. *J. Am. Chem. Soc.* **119**, 8720–8721 (1997).
12. M. Cheng, Q. Liu, G. Ju, Y. Zhang, L. Jiang, F. Shi, Bell-shaped superhydrophilic-superhydrophobic-superhydrophilic double transformation on a pH-responsive smart surface. *Adv. Mater.* **26**, 306–310 (2014).
13. F. Xia, L. Feng, S. Wang, T. Sun, W. Song, W. Jiang, L. Jiang, Dual-responsive surfaces that switch between superhydrophilicity and superhydrophobicity. *Adv. Mater.* **18**, 432–436 (2006).
14. J. R. Matthews, D. Tuncel, R. M. J. Jacobs, C. D. Bain, H. L. Anderson, Surfaces designed for charge reversal. *J. Am. Chem. Soc.* **125**, 6428–6433 (2003).
15. T. Sun, G. Wang, L. Feng, B. Liu, Y. Ma, L. Jiang, D. Zhu, Reversible switching between superhydrophilicity and superhydrophobicity. *Angew. Chem. Int. Ed. Engl.* **43**, 357–360 (2004).
16. M. A. Stuart, W. T. S. Huck, J. Genzer, M. Muller, C. Ober, M. Stamm, G. B. Sukhorukov, I. Szleifer, V. V. Tsukruk, M. Urban, F. Winnik, S. Zauscher, I. Luzinov, S. Minko, Emerging applications of stimuli-responsive polymer materials. *Nat. Mater.* **9**, 101–113 (2010).
17. L. Xu, W. Chen, A. Mulchandani, Y. Yan, Reversible conversion of conducting polymer films from superhydrophobic to superhydrophilic. *Angew. Chem. Int. Ed. Engl.* **44**, 6009–6012 (2005).
18. O. Azzaroni, A. A. Brown, W. T. S. Huck, Tunable wettability by clicking counterions into polyelectrolyte brushes. *Adv. Mater.* **19**, 151–154 (2007).
19. B. S. Lee, Y. S. Chi, J. K. Lee, I. S. Choi, C. E. Song, S. K. Namgoong, S.-g. Lee, Imidazolium ion-terminated self-assembled monolayers on Au: Effects of counteranions on surface wettability. *J. Am. Chem. Soc.* **126**, 480–481 (2004).
20. H. S. Lim, S. G. Lee, D. H. Lee, D. Y. Lee, S. Lee, K. Cho, Superhydrophobic to superhydrophilic wetting transition with programmable ion-pairing interaction. *Adv. Mater.* **20**, 4438–4441 (2008).
21. J. Lahann, S. Mitragotri, T. N. Tran, H. Kaido, J. Sundaram, I. S. Choi, S. Hoffer, G. A. Somorjai, R. Langer, A reversibly switching surface. *Science* **299**, 371–374 (2003).
22. Z. Wang, L. Ci, L. Chen, S. Nayak, P. M. Ajayan, N. Koratkar, Polarity-dependent electrochemically controlled transport of water through carbon nanotube membranes. *Nano Lett.* **7**, 697–702 (2007).
23. W. Barthlott, C. Neinhuis, Purity of the sacred lotus, or escape from contamination in biological surfaces. *Planta* **202**, 1–8 (1997).
24. A. Lafuma, D. Quéré, Superhydrophobic states. *Nat. Mater.* **2**, 457–460 (2003).
25. T.-S. Wong, S. H. Kang, S. K. Y. Tang, E. J. Smythe, B. D. Hatton, A. Grinthal, J. Aizenberg, Bioinspired self-repairing slippery surfaces with pressure-stable omniphobicity. *Nature* **477**, 443–447 (2011).
26. S. Anand, A. T. Paxson, R. Dhiman, J. D. Smith, K. K. Varanasi, Enhanced condensation on lubricant-impregnated nanotextured surfaces. *ACS Nano* **6**, 10122–10129 (2012).
27. X. Dai, N. Sun, S. O. Nielsen, B. B. Stogin, J. Wang, S. Yang, T.-S. Wong, Hydrophilic directional slippery rough surfaces for water harvesting. *Sci. Adv.* **4**, eaaq0919 (2018).
28. S. Yang, N. Sun, B. B. Stogin, J. Wang, Y. Huang, T.-S. Wong, Ultra-antireflective synthetic brochosomes. *Nat. Commun.* **8**, 1285 (2017).
29. Y. Wang, L. Zhao, Y. Zhao, W. Y. Wang, Y. Liu, C. Gu, J. Li, G. Zhang, T. J. Huang, S. Yang, Electrocarving during electrodeposition growth. *Adv. Mater.* **30**, e1805686 (2018).
30. M. W. J. Prins, W. J. Welters, J. W. Weekamp, Fluid control in multichannel structures by electrocapillary pressure. *Science* **291**, 277–280 (2001).
31. R. A. Hayes, B. J. Feenstra, Video-speed electronic paper based on electrowetting. *Nature* **425**, 383–385 (2003).
32. Z. Tan, H. Abe, S. Ohara, Ordered deposition of Pd nanoparticles on sodium dodecyl sulfate-functionalized single-walled carbon nanotubes. *J. Mater. Chem.* **21**, 12008–12014 (2011).
33. L. J. Christopher, L. A. Estroff, J. K. Kriebel, R. G. Nuzzo, G. M. Whitesides, Self-assembled monolayers of thiolates on metals as a form of nanotechnology. *Chem. Rev.* **105**, 1103–1169 (2010).
34. A. B. Zrimsek, N. Chiang, M. Mattei, S. Zaleski, M. O. McAnally, C. T. Chapman, A. I. Henry, G. C. Schatz, R. P. Van Duyne, Single-molecule chemistry with surface- and tip-enhanced Raman spectroscopy. *Chem. Rev.* **117**, 7583–7613 (2017).
35. D. Liu, L. Liu, L. Ji, Z. Qi, Y. Xia, Y. Song, D. Dong, Z. Li, R. Liu, B. Liu, D. Sun, D. Liu, Detection and plasma assisted degradation of dye on reusable gold coated tungsten nanofuzz array surface-enhanced Raman scattering substrate. *Appl. Surf. Sci.* **469**, 262–268 (2019).
36. X. Li, H. Tian, J. Shao, Y. Ding, X. Chen, L. Wang, B. Lu, Decreasing the saturated contact angle in electrowetting-on-dielectrics by controlling the charge trapping at liquid-solid interfaces. *Adv. Funct. Mater.* **26**, 2994–3002 (2016).
37. S. Nie, S. R. Emory, Probing single molecules and single nanoparticles by surface-enhanced raman scattering. *Science* **275**, 1102–1106 (1997).
38. K. Kneipp, Y. Wang, H. Kneipp, L. T. Perelman, I. Itzkan, R. R. Dasari, M. S. Feld, Single molecule detection using surface-enhanced Raman scattering (SERS). *Phys. Rev. Lett.* **78**, 1667–1670 (1997).
39. R. Wen, Q. Li, J. Wu, G. Wu, W. Wang, Y. Chen, X. Ma, D. Zhao, R. Yang, Hydrophobic copper nanowires for enhancing condensation heat transfer. *Nano Energy* **33**, 177–183 (2017).
40. A. R. Parker, C. R. Lawrence, Water capture by a desert beetle. *Nature* **414**, 33–34 (2001).
41. A. K. Epstein, T.-S. Wong, R. A. Belisle, E. M. Boggs, J. Aizenberg, Liquid-infused structured surfaces with exceptional anti-biofouling performance. *Proc. Natl. Acad. Sci. U.S.A.* **109**, 13182–13187 (2012).

Acknowledgments

Funding: We acknowledge funding support by the Zhejiang Provincial Natural Science Foundation of China (LR19E010001), the National Key Research and Development Program of China (2018YFB0703803), and the National Science Foundation of China (51702283). **Author contributions:** S.Y. conceived the idea. S.Y. and Y.L. designed the experiments. Y.L. and L.Z. performed materials fabrication and characterizations. S.Y., Y.L., and J.L. conducted data analysis. Y.L. and S.Y. wrote the paper. All authors contributed to paper revision. **Competing interests:** The authors declare that they have no competing interests. **Data and materials availability:** All data needed to evaluate the conclusions in the paper are present in the paper and/or the Supplementary Materials. Additional data related to this paper may be requested from the authors.

Submitted 16 February 2019
Accepted 16 September 2019
Published 1 November 2019
10.1126/sciadv.aax0380

Citation: Y. Liu, L. Zhao, J. Lin, S. Yang, Electrodeposited surfaces with reversibly switching interfacial properties. *Sci. Adv.* **5**, eaax0380 (2019).